



Role of HMGB1 in TNF- α Combined with Z-VAD-fmk-Induced L929 Cells Necroptosis

Can Yu¹ · Zhao Lei² · Xia Li³ · Li-Hua Huang⁴ · Zhi-Qiang Li² · Hong-Wei Zhu² · Duo Han² · Hui Huang² · Xiao Yu² 

Received: 24 December 2020 / Accepted: 6 July 2021 / Published online: 29 July 2021

© The Author(s), under exclusive licence to Springer Science+Business Media, LLC, part of Springer Nature 2021, corrected publication 2021

Abstract

The present study established a necroptosis model in vitro and investigated the role of HMGB1 in cell necroptosis. A combination of tumor necrosis factor- α and z-VAD-fmk was used to induce necroptosis in L929 cells with necroptosis inhibitor necrostatin-1 applied as an intervention. Flow cytometry and transmission electron microscopy (TEM) were used to measure cell necroptosis. Western blotting assay was applied to detect the expression of receptor-interacting serine/threonine-protein kinase 3 (RIPK3), mixed lineage kinase domain-like pseudokinase (MLKL) and HMGB1. Co-immunoprecipitation (Co-IP) assay was used to confirm the interaction between HMGB1 and RIPK3. Our study demonstrated that HMGB1 migrated from the nucleus to the cytoplasm at the onset of necroptosis and was subsequently released passively to the extracellular matrix. Further experiments determined that the binding of HMGB1 with RIPK3 in the cytoplasm was loose during necroptosis. By contrast, when necroptosis was inhibited, the interaction in the cytoplasm was tight suggesting that this association between HMGB1 and RIPK3 might affect its occurrence. In conclusion, the transfer of HMGB1 from nucleus to cytoplasm, and its interaction with RIPK3 might be potentially involved in necroptosis.

Keywords High mobility group protein 1 · Necroptosis · Receptor interacting serine/threonine kinase 3 · Mixed lineage kinase domain-like pseudokinase

Can Yu and Zhao Lei are the co-first authors.

✉ Xiao Yu
yuxiaoyx90@163.com

Extended author information available on the last page of the article

Introduction

Necroptosis is a regulated form of cell death, distinct from apoptosis, autophagy and necrosis, acting as a defense mechanism against viruses through the release of inflammatory mediators. Necroptosis also plays a role in various inflammatory diseases and the study of necroptotic pathways may provide novel therapeutic targets (Wu et al. 2017; Peng et al. 2017; Caccamo et al. 2017; Galluzzi et al. 2017). However, the underlying molecular mechanisms of necroptosis are complex and have yet to be fully elucidated.

Damage-associated molecular patterns (DAMPs) are a class of endogenous molecules that exert critical physiological functions and biological effects within the cell. When released extracellularly, DAMPs bind to their associated membrane receptors, resulting in an imbalance of the inflammatory reaction, causing disorder to the immune response (Shi et al. 2003). This may lead to necroptosis. The role of high mobility group protein 1 (HMGB1), a vital member of the DAMPs family, in inflammation is under intensive focus; however, the underlying mechanism of its action is complex and needs further investigation. In the nucleus, HMGB1 binds to DNA and effectuates DNA recombination, gene transcription and cell division. Several studies have explored the role of HMGB1 in the cytoplasm in the process of autophagy (Kang et al. 2014; Linkermann and Green 2014; Sun et al. 2012). Extracellularly, HMGB1 acts as an inflammatory mediator or as a receptor ligand and is involved in intercellular signaling transduction (Kang et al. 2014). Various pathophysiological functions of HMGB1 indicate that the protein may participate in necroptosis (Xie et al. 2013). However, deeper insights are still needed to elucidate the role of HMGB1 in necroptosis process.

In the classical necroptosis pathway, TNF- α combined with caspase inhibitor z-VAD-fmk, promotes receptor-interacting serine/threonine-protein kinase (RIPK) 1 to interact with RIPK3 and recruits other related molecules to form a necrosome, a key step in the initial phase of necroptosis (Linkermann and Green 2014). Necrostatin-1 (Nec-1) specifically blocks necroptosis via suppression of the kinase activity of RIPK1 and RIPK3 by acting at their active sites and blocking their mutual phosphorylation (Murphy et al. 2013; Cai et al. 2014; Chen et al. 2014). Mixed lineage kinase domain-like protein (MLKL) is a specific substrate of RIPK3 involved in executing necroptosis. Upon autophosphorylation, RIPK3 binds to MLKL via the kinase domain and phosphorylates the corresponding sites in different MLKL kinase-like domains, which in turn, promote necroptosis (Sun et al. 2012; Xie et al. 2013). Phosphorylated (p) MLKL recruits and phosphorylates PGAM family member 5, a protein present in the mitochondria (Chen et al. 2015). Phosphorylated PGAM is then dephosphorylated and activates the mitochondrial cleavage protein Drp1, which in turn, triggers mitochondrial cleavage and the generation of reactive oxygen species, eventually leading to cell necroptosis (Sun et al. 2012; Wang et al. 2012). p-MLKL monomers also bind to each other via their N-terminal functional regions to form homo-oligomers that are transferred to the internal side of the membrane from the cytoplasm via lipid

rafts. This process increases Na^+ and Ca^{2+} influx causing cell necroptosis (Murphy et al. 2013; Cai et al. 2014; Chen et al. 2014; Wang et al. 2014). However, up to now, few studies focused on the interaction between HMGB1 and RIPK3/MLKL signaling in necroptosis.

In the present study, a reliable necroptosis model was established and the role of HMGB1 as well as its relationship with RIPK3/MLKL signaling was preliminarily investigated. This research might provide novel understanding for molecular mechanisms of HMGB1 in necroptosis.

Materials and Methods

Cell Culture and Treatment

The L929 mouse fibroblast cell line was purchased from the Cell Research Center of Xiangya Medical College of Central South University. Briefly, cells were cultured in Dulbecco's modified Eagle's medium (DMEM, HyClone; GE Healthcare Life Sciences) containing 10% fetal bovine serum (FBS; Gibco; Thermo Fisher Scientific, Inc.) and 1% PS (100 IU/ml penicillin, 100 $\mu\text{g}/\text{ml}$ streptomycin) in an incubator at 37 °C and 5% CO_2 .

L929 fibroblast cells are a cell line commonly used to study the cytotoxicity of TNF- α (Chen et al. 2015). For establish of the necroptosis model, the L929 cells were treated with 10 ng/ml recombinant mouse (rm) TNF- α (cat. no. C315-01A; Proteintech Group Inc.) at 37 °C for 24 h, following by treatment with 10 μM pan-caspase inhibitor z-VAD-fmk (Cat. No. S7023; Selleck Chemicals). For inhibition of necroptosis, the necroptosis model cells were treated with 30 μM necroptosis inhibitor Nec-1 (Cat. No. S8037; Selleck Chemicals) for 1 h at 37 °C. The cells were divided into following groups: Control group (untreated cells), TNF- α group (L929 cells treated with 10 ng/ml TNF- α only), necroptosis group (L929 cells treated with 10 ng/ml TNF- α and 10 μM z-VAD-fmk) and necroptosis inhibition group (L929 cells treated with 10 ng/ml TNF- α , 10 μM z-VAD-fmk and 30 μM Nec-1).

Flow Cytometry Detection for Measurement of Cell Necroptosis

For measurement of cell necroptosis, flow cytometry assay was conducted. Briefly, after centrifugation at room temperature for 10 min at 800 x g, cells were collected, washed with phosphate buffer saline (PBS) and resuspended in binding buffer (cat. no. KGF 00; Keygen Biotech Co. Ltd; 300 μl). The cells were then stained using an Annexin V-FITC/PI double staining flow cytometry detection kit (Cat. No. KGA 107; Keygen Biotech Co. Ltd.) strictly according to the manufacturer's instruction. A flow cytometer (FACSCalibur, BD Biosciences) was used to analyze the cell necrosis (CellQuest and WinMDI 2.9 *software* packages; BD Biosciences).

Cell Morphology by Transmission Electron Microscopy (TEM)

For observing cell morphology by TEM, briefly, cells in the logarithmic growth phase were harvested after centrifugation at 450 x g at room temperature for 5 min. Then, cells were fixed with 1% glutaraldehyde and 1% OsO₄ at room temperature for 1 h, dehydrated in alcohol and infiltrated with a mixture of embedding agent and acetone (V/V = 1:1) at room temperature for 1 h. After embedded in an embedding agent at 70 °C overnight and sliced into 50 nm, cells were stained with uranyl *acetate* and lead citrate for 15 min, and were observed using a HT7700 transmission electron microscope (Hitachi, Ltd.). The images were photographed with a magnification of ×400,000.

Western Blotting Analysis

For western blotting analysis, proteins were extracted using RIPA buffer (Beyotime Institute of Biotechnology). The nuclear and cytoplasmic proteins were collected using a Nuclear/Cytosol Fractionation Kit (BioVision Research Products, Mountain View, CA, USA). The protein concentration was detected using a bicinchoninic acid protein concentration kit (Sigma-Aldrich; Merck KGaA). An equivalent of 50 µg protein was subjected to 10% SDS-PAGE, transferred to polyvinylidene difluoride membranes, and blocked in 5% skimmed-milk in TBST buffer at room temperature for 1 h. Samples were then incubated with primary antibodies against RIPK3 (Cat. No. 17563-1-ap; Proteintech Group Inc.; 1:500), HMGB1 (Cat. No. 10829-1-ap; Proteintech Group Inc.; 1:1,000); β-actin (Cat. No. 600008-1; Proteintech Group Inc.; 1:4,000), proliferating cell nuclear antigen (PCNA; Cat. No. CST 3656S; Cell Signaling Technology, Inc.; 1:2,000), p-MLKL (cat. no. ab196436; Abcam; 1:1,000) and MLKL (Cat. No. 21066-1-AP; Proteintech Group Inc.; 1:750) at 4 °C overnight, following by incubation with horseradish peroxidase (HRP)-conjugated secondary antibody (Cat. No. SA00001-2; Proteintech Group Inc.; 1:3,000) at 37 °C for 1 h. Finally, the immunoreactive bands were visualized using the Enhanced Chemiluminescence kit (Thermo Fisher Scientific, Inc.) by the Image Quant 350 Gel Protein Imaging System (version 1.0.2; GE Healthcare). The ratio of the target and reference protein gray values was determined and compared between the groups using Image Analysis Software (version 7.0; GE Healthcare).

Enzyme Linked Immunosorbent Assay (ELISA) Detection of HMGB1

For measurement of the HMGB1 levels in cell supernatant, briefly, cells were suspended with density of 1×10^8 cells/ml. The HMGB1 levels were determined by ELISA using an HMGB-1 ELISA kit (Cat. No. LS-F30785; LifeSpan Biosciences Co., Ltd.) according to the manufacturer's instruction. The optical absorbance was measured at 450 nm within 15 min of experimentation.

Co-Immunoprecipitation (Co-IP) Assay to Assess the Interaction Between HMGB1 and RIPK3

The cells of each group were treated with RIPA buffer and incubated with the HMGB1 antibody (Cat. No. 10829-1-ap; Proteintech Group Inc.; 1:500) at 4 °C overnight. The negative control group was incubated with the Ig antibody. Then, 20 μ l protein A agarose beads were washed with the lysate three times and were centrifuged at 1800 \times g at room temperature for 3 min. The pretreated Protein A agarose beads were added into the cell lysate, which was then incubated with antibody overnight at 4 °C for 2 h to form the antibody-Protein A agarose complex. The positive control group was a solution containing the HMGB1 and RIPK3 proteins. Subsequently, the complex was analyzed by western blotting as described above. The same antibodies as in western blotting were used. Dilutions of the primary antibodies were as follows: 1:1000 for HMGB1 and 1:300 for RIPK3. The secondary antibody was utilized at a 1:3000 dilution.

Statistical Analysis

All experiments were repeated in triplicate independently. Data are presented as the mean \pm standard deviation (SD). One-way analysis of variance (ANOVA) was used for multiple comparisons among the groups followed by Tukey post hoc test. $P < 0.05$ was considered to indicate a statistically significant difference. All calculations were made using SPSS 20.0 (SPSS Inc., Chicago, USA).

Results

TNF- α and z-VAD-fmk Co-Treatment to Establish a Necroptosis Model

To establish the necroptosis model, cells were treated with 10 ng/ml TNF- α and 10 μ M z-VAD-fmk. The proportion of living cells and the PI-positive cells (including necrotic and late apoptotic cells) in different experimental groups was determined by flow cytometry (Fig. 1A). Compared with the control (98.82%) and TNF- α (78.63%) groups, the proportion of living cells in the necroptosis group (61.77%) decreased significantly, while necroptosis inhibition (96.39%) reversed this effect (Fig. 1B). By contrast, the ratio of PI-positive cells in the necroptosis group (32.76%) increased significantly compared with the control (0.60%) and TNF- α (16.16%) groups, while necroptosis inhibition significantly decreased PI-positive cells (1.76%) (Fig. 1C). These results indicated the successful establishment of the necroptosis model.

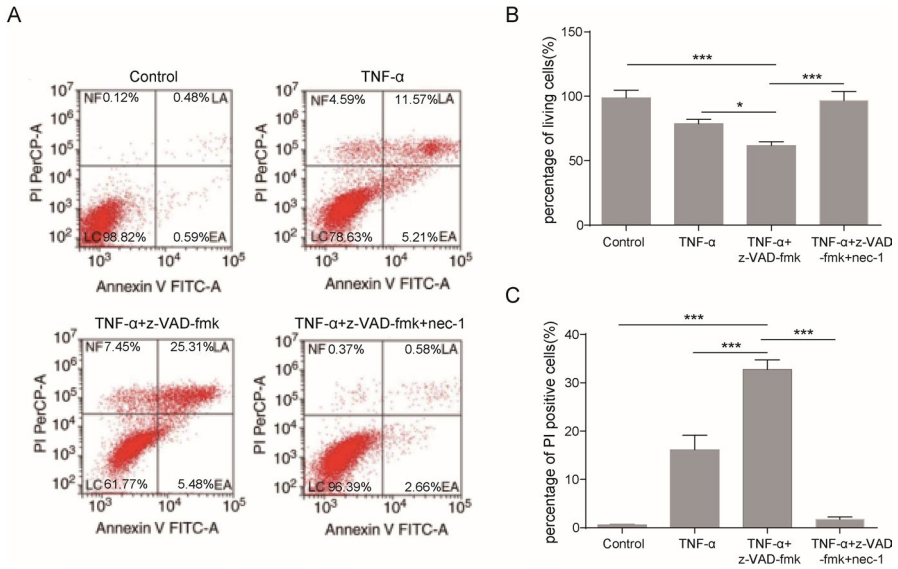


Fig. 1 Detection of cell death in the models by flow cytometry. **A** Flow cytometry dot plots. **B** Proportion of live cells (FITC⁻/PI⁻) in control, TNF- α , TNF- α + z-VAD-fmk and TNF- α + z-VAD-fmk + nec-1 groups. **C** Percentage of PI⁺ cells in these four groups. Data are expressed as the mean \pm standard deviation. *N* = 3; **P* < 0.05, ***P* < 0.01, ****P* < 0.001. TNF- α , tumor necrosis factor- α ; PI, propidium iodide; FITC fluorescein isothiocyanate, NF nuclear fragment, LA late apoptosis, LC live cells, EA early apoptosis

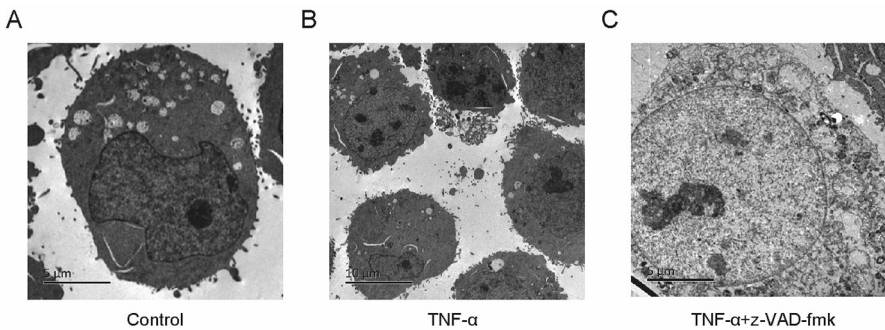


Fig. 2 Observation of the morphological changes in necroptotic L929 cells by electron microscopy. **A** Representative image of a normal cell with continuous cell membrane and intact nuclear membrane. **B** Representative image of an apoptotic cell with the cell volume decreased, cytoplasm condensed and the chromatin condensed into blocks, scattered in the nucleus and moved under the nuclear membrane. **C** Representative image of a necroptotic cell demonstrating swollen nucleus and nuclear membrane, disintegrated cell membrane and vacuolated cytoplasm. Magnification, $\times 400,000$

Morphological Changes in Necroptotic L929 Cells were Observed by Electron Microscopy

To further investigate the morphological changes to L929 cells following TNF- α and z-VAD-fmk co-treatment, cells were observed under TEM. As shown in Fig. 2, in normal cells, the cell membrane was continuous and the nuclear membrane was intact (Fig. 2A). In apoptotic cells, the cell volume was decreased, cytoplasm was condensed and the chromatin was condensed into blocks which scattered in the nucleus and attached to the periphery of nuclear membrane (Fig. 2B). However, in necroptotic cells, the nucleus swelled, the cell membrane and nuclear membrane disintegrated and the cytoplasm was vacuolated (Fig. 2C). All these results demonstrated the morphology change of necroptotic cells and further confirm the successful establishment of the necroptosis model.

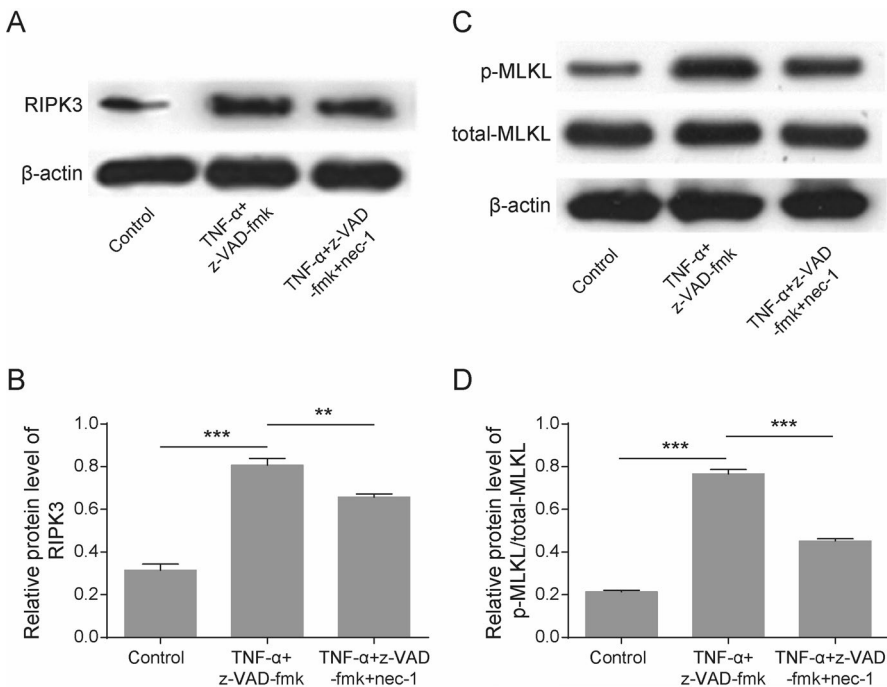


Fig. 3 Key signaling molecules in the pathway of necroptosis. **A** The expression of RIPK3 and the p-MLKL to total MLKL ratio was determined by western blotting. Compared with the control group, TNF- α combined with z-VAD-fmk (necroptosis group) significantly increased the expression of **B** RIPK3 and **C-D** the p-MLKL/MLKL ratio. Application of necroptosis inhibitor Nec-1 downregulated the RIPK3 and p-MLKL/MLKL expression in the necroptosis group. Data are expressed as the mean \pm standard deviation. $N=3$; ** $P < 0.01$, *** $P < 0.001$. RIPK receptor-interacting serine/threonine-protein kinase, *p* phosphorylated, MLKL mixed lineage kinase domain-like protein, TNF- α tumor necrosis factor- α

RIPK3 and MLKL were Key Signaling Molecules in the Necroptosis Pathway

Then, protein expression of RIPK3 and MLKL were determined in different groups of cells. It was found that after the cells were stimulated with TNF- α and z-VAD-fmk for 24 h, the protein levels of RIPK3 and the ratio of p-MLKL/total-MLKL were significantly increased compared with the control group (Fig. 3). Meanwhile, application of the necroptosis inhibitor Nec-1 reduced RIPK3 expression and the ratio of p-MLKL/total-MLKL in the necroptosis inhibition group compared to the necroptosis group (Fig. 3), suggesting that RIPK3 and MLKL might be associated with necroptosis process.

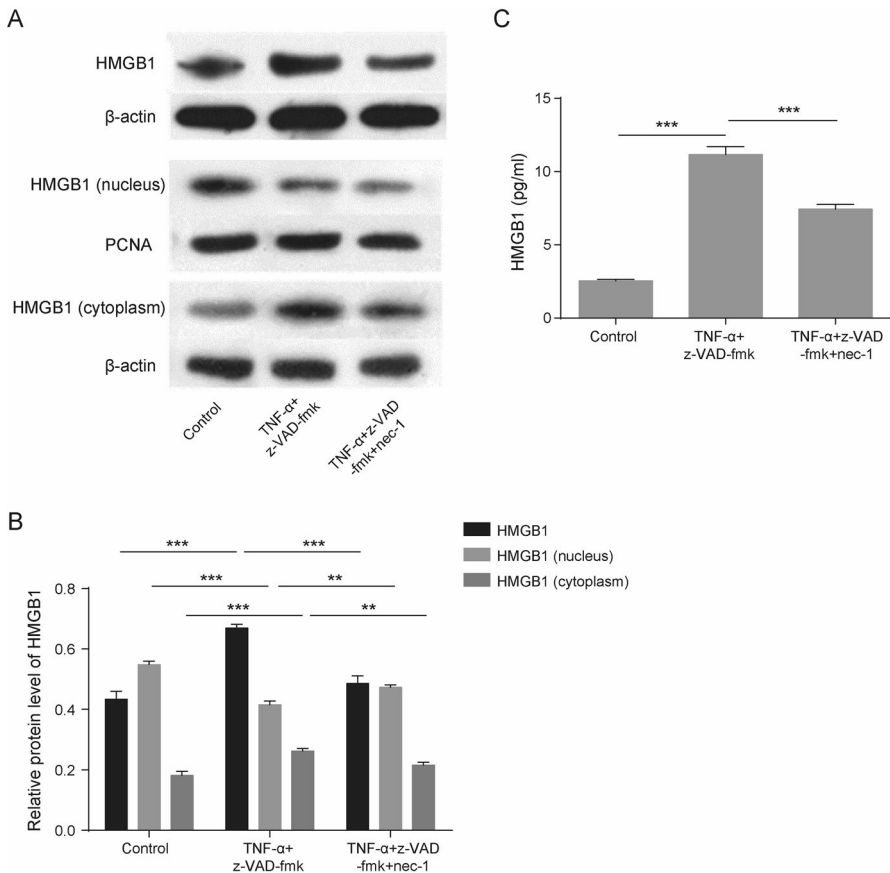


Fig. 4 Expression of HMGB1 in necroptosis. **A** Western blot analysis was used to detect the protein expression of HMGB1 in total and in the nucleus and cytoplasm individually. **B** The relative protein expression levels of total HMGB1 and in the nucleus and cytoplasm during necroptosis and necroptosis inhibition. **C** ELISA was used to determine the release level of HMGB1 in the serum during necroptosis. Data are expressed as the mean \pm standard deviation. $N=3$; $**P<0.01$, $***P<0.001$. HMGB1, high mobility group protein 1; PCNA, proliferating cell nuclear antigen

HMGB1 was Differentially Expressed in the Nucleus and Cytoplasm in Necroptosis

Next, the role of HMGB1 in necroptosis was also investigated. Results showed HMGB1 expression was significantly increased in necrotic L929 cells compared with the control cells (Fig. 4A–B). Further analysis indicated that when necroptosis occurred, the expression of HMGB1 in the nucleus decreased significantly while the expression in the cytoplasm was significantly increased. Besides, the protein levels of HMGB1 in both nucleus and cytoplasm were markedly decreased following the addition of the necroptosis inhibitor. Additionally, HMGB1 concentration in cultural medium was also increased by necroptosis induction, which was suppressed by necroptosis inhibition (Fig. 4C). These results indicated that HMGB1 was also associated with necroptosis.

The Interaction Between HMGB1 and RIPK3 was Weakened in Necroptosis

Finally, the interaction between HMGB1 and RIPK3 was confirmed and the alteration was determined. As shown in Fig. 5, in necroptosis cells, the interaction between HMGB1 and RIPK3 was remarkably weakened. After the application of a necroptosis inhibitor, the interaction between HMGB1 and RIPK3 was significantly enhanced, suggesting the interaction between HMGB1 and RIPK3 was affected by the necroptosis process.

Discussion

Despite numerous studies and long-term knowledge for cell necroptosis, the underlying molecular mechanisms for necroptosis are still unclear. HMGB1 is a newly found inflammation related factor, which participates in many diseases and bio-processes. However, up to now, few studies focused on role of HMGB1 in cell necroptosis. In the present study, we demonstrated that the expression of HMGB1

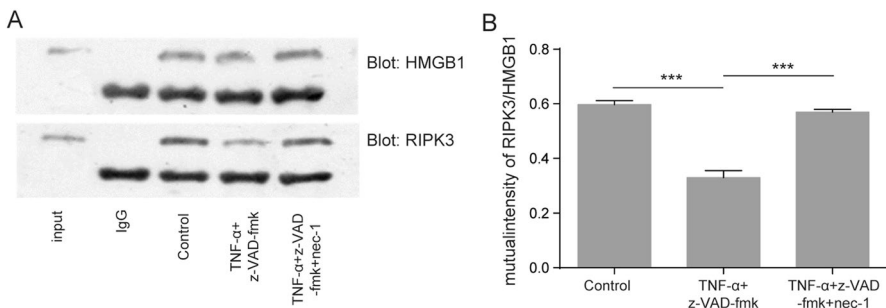
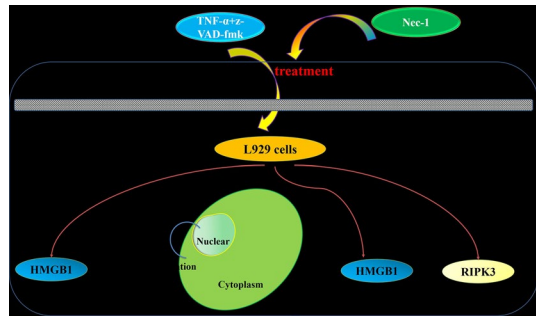


Fig. 5 The interaction between HMGB1 and RIPK3 during necroptosis and necroptosis inhibition was explored by co-immunoprecipitation. **A** The western blot results. **B** The ratio of immunoprecipitated RIPK3/HMGB1 represents the strength of interaction between HMGB1 and RIPK3. Data are expressed as the mean \pm standard deviation. $N=3$; $***P < 0.001$. *IgG* immunoglobulin G, *HMGB1* high mobility group protein 1, *RIPK* receptor-interacting serine/threonine-protein kinase

Fig. 6 Possible molecular mechanism for HMGB1 in TNF- α combined with z-VAD-fmk-induced L929 cells necroptosis



was upregulated in cell cytoplasm and decreased in nucleus in necrotic cells, and its interaction with RIPK3 and HMGB1 might be involved in this process (Fig. 6).

In the present research, we used TNF- α and pan-caspase inhibitor z-VAD-fmk co-treatment to induce cell necroptosis. TNF- α and z-VAD-fmk have been used to induce necroptosis model in various studies. In an early research, Günther et al. used TNF- α to induce cell necroptosis and found knockdown of caspase-8 facilitated the cell necroptosis in epithelial cells (Günther et al. 2011). In a recent study, Li et al. used z-VAD-fmk to improve endotoxic shock by inducing necroptosis of macrophages (Li et al. 2019). In another study, the authors used both TNF- α and z-VAD-fmk to induce necroptosis in renal epithelial cells (Liang et al. 2014). In our research, we also successfully established the necroptosis model using TNF- α and z-VAD-fmk. Besides, the Nec-1 was used to inhibit necroptosis. In 2005, Degtarev et al. (Deng et al. 2019) showed that the small molecule Nec-1 specifically blocked necroptosis, caspase-induced non-dependent cell death, which was consistent with our results.

HMGB1 is released extracellularly primarily through active secretion by inflammatory cells and passive release by necrotic cells. When monocytes, macrophages, and dendritic cells are stimulated, HMGB1 is released in a dose- and time-dependent manner (Wang et al. 2004). The role of HMGB1 in inflammation has been demonstrated in many studies. It has been found HMGB1 is activated in inflammation response and high levels of HMGB1 promote inflammation (Soliman et al. 2020; Deng et al. 2019; Steinle 2020). Except for role of HMGB1 in inflammation, HMGB1 is also considered to play important roles in necroptosis. It was found the inhibition of HMGB1 led to improvement of hypoxia/reoxygenation-induced necroptosis in cardiomyocytes (Chen et al. 2019). In a more recent research, Simpson et al. also demonstrated that necroptosis induced by respiratory syncytial virus was associated with the increased release of HMGB1 (Simpson et al. 2020). However, despite these studies, role of HMGB1 in cell necroptosis needs further elaboration. The present study found HMGB1 expression decreased in the nucleus but began to increase in the cytoplasm. This phenomenon confirmed the release of HMGB1 from the nucleus to the cytoplasm during the onset of necroptosis. This finding suggested that by reducing the occurrence of necroptosis, the release of HMGB1 could be reduced, which controls the extracellular HMGB1-induced pathogenesis.

Accumulating evidence demonstrated that RIPK1 is not a critical factor in necroptosis, while RIPK3 expression is an essential component in the process of forming various inductive necrosomes in the initial stage of necroptosis (Han et al. 2011). Previous studies have demonstrated that when RIPK3 was knocked-out, RIPK1 could only mediate the apoptotic pathway, and RIPK1 mediated necroptosis only in the presence of RIPK3 (Cho et al. 2009; He et al. 2009). After the expression of RIPK3 was downregulated, cell necroptosis was inhibited but apoptosis was not affected (Cho et al. 2009). These studies indicated that RIPK3 is the key factor in the pathway of necroptosis, and thus, it can be used as a specific marker of necroptosis. The present study determined that HMGB1 bond to RIPK3 in the cytoplasm in normal cells and the interaction between HMGB1 and RIPK3 was weakened in cell necroptosis, indicating that the binding of HMGB1 and RIPK3 might exert a protective role in the process of necroptosis. However, more studies are still needed to provide deeper insights for how the interaction between HMGB1 and RIPK influences necroptosis.

In summary, the present study determined that necroptosis may cause extracellular release of the DAMP molecule HMGB1. It was identified that HMGB1 had a different role according to the localization in the nucleus, cytoplasm or outside of the cell; however, the underlying mechanism requires further investigation. The present findings demonstrated that HMGB1 might be useful for identifying novel therapeutic approaches that regulate necroptosis and may be a novel biomarker for the pathogenesis and progression of necrosis.

Acknowledgements Not applicable.

Funding This work was supported by the National Natural Science Foundation of China (Grant No. 81873589), and by the Hunan Natural Science Foundation Youth Fund Project (Grant No. 2020JJ5853, No. 2021JJ40952).

Data Availability All data generated or analyzed during this study are included in this published article.

Declarations

Conflict of interest The authors declare that they have no competing interests.

References

- Caccamo A, Branca C, Piras IS, Ferreira E, Huentelman MJ, Liang WS et al (2017) Necroptosis activation in Alzheimer's disease. *Nat Neurosci* 20(9):1236–1246
- Cai Z, Jitkaew S, Zhao J, Chiang HC, Choksi S, Liu J et al (2014) Plasma membrane translocation of trimerized MLKL protein is required for TNF-induced necroptosis. *Nat Cell Biol* 16(1):55–65
- Chen X, Li W, Ren J, Huang D, He WT, Song Y et al (2014) Translocation of mixed lineage kinase domain-like protein to plasma membrane leads to necrotic cell death. *Cell Res* 24(1):105–121
- Chen G, Cheng X, Zhao M, Lin S, Lu J, Kang J et al (2015) RIP1-dependent Bid cleavage mediates TNF α -induced but caspase-3-independent cell death in L929 fibroblastoma cells. *Apoptosis* 20(1):92–109
- Chen J, Jiang Z, Zhou X, Sun X, Cao J, Liu Y et al (2019) Dexmedetomidine preconditioning protects cardiomyocytes against hypoxia/reoxygenation-induced necroptosis by inhibiting HMGB1-mediated inflammation. *Cardiovasc Drugs Ther* 33(1):45–54

- Cho YS, Challa S, Moquin D, Genga R, Ray TD, Guildford M et al (2009) Phosphorylation-driven assembly of the RIPK1-RIPK3 complex regulates necroptosis and virus-induced inflammation. *Cell* 137(6):1112–1123
- Deng M, Scott MJ, Fan J, Billiar TR (2019) Location is the key to function: HMGB1 in sepsis and trauma-induced inflammation. *J Leukoc Biol* 106(1):161–169
- Galluzzi L, Kepp O, Chan FK, Kroemer G (2017) Necroptosis: mechanisms and relevance to disease. *Annu Rev Pathol* 12:103–130
- Günther C, Martini E, Wittkopf N, Amann K, Weigmann B, Neumann H et al (2011) Caspase-8 regulates TNF- α -induced epithelial necroptosis and terminal ileitis. *Nature* 477(7364):335–339
- Han J, Zhong CQ, Zhang DW (2011) Programmed necrosis: backup to and competitor with apoptosis in the immune system. *Nat Immunol* 12(12):1143–1149
- He SD, Wang L, Miao L, Wang T, Du FH, Zhao LP, et al (2009) Receptor interacting protein kinase-3 determines cellular necrotic response to TNF- α . *Cell* 137(6):1100–1111
- Kang R, Chen R, Zhang Q, Hou W, Wu S, Cao L et al (2014) HMGB1 in health and disease. *Mol Aspects Med* 40:111–116
- Li X, Yao X, Zhu Y, Zhang H, Wang H, Ma Q et al (2019) The caspase inhibitor Z-VAD-FMK alleviates endotoxic shock via inducing macrophages necroptosis and promoting MDSCs-mediated inhibition of macrophages activation. *Front Immunol* 10:1824
- Liang X, Chen Y, Zhang L, Jiang F, Wang W, Ye Z et al (2014) Necroptosis, a novel form of caspase-independent cell death, contributes to renal epithelial cell damage in an ATP-depleted renal ischemia model. *Mol Med Rep* 10(2):719–724
- Linkermann A, Green DR (2014) Necroptosis. *New Eng J Med* 370:455–465
- Murphy JM, Czabotar PE, Hildebrand JM, Lucet IS, Zhang JG, Alvarez-Diaz S et al (2013) The pseudokinase MLKL mediates necroptosis via a molecular switch mechanism. *Immunity* 39(3):443–453
- Peng SY, Xu JM, Ruan W, Li SB, Xiao F (2017) PPAR- γ activation prevents septic cardiac dysfunction via inhibition of apoptosis and necroptosis. *Oxid Med Cell Longev* 2017:8326749
- Shi Y, Evans JE, Rock KL (2003) Molecular identification of a danger signal that alerts the immune system to dying cells. *Nature* 425(6957):516–521
- Simpson J, Loh Z, Ullah MA, Lynch JP, Werder RB, Collinson N et al (2020) Respiratory syncytial virus infection promotes necroptosis and HMGB1 release by airway epithelial cells. *Am J Respir Crit Care Med* 201(11):1358–1371
- Soliman NA, Abdel Ghafar MT, El Kolalely RM, Hafez YM, Abo Elgheit RE, Atef MM (2020) Cross talk between Hsp72, HMGB1 and RAGE/ERK1/2 signaling in the pathogenesis of bronchial asthma in obese patients. *Mol Biol Rep* 47:4109–4116
- Steinle JJ (2020) Role of HMGB1 signaling in the inflammatory process in diabetic retinopathy. *Cell Signal* 73:109687
- Sun LM, Wang HY, Wang ZG, He SD, Chen S, Liao DH et al (2012) Mixed lineage kinase domain-like protein mediates necrosis signaling downstream of RIP3 kinase. *Cell* 148(1–2):213–227
- Wang H, Liao H, Ochani M, Justiniani M, Lin X, Yang L et al (2004) Cholinergic agonists inhibit HMGB1 release and improve survival in experimental sepsis. *Nat Med* 10(11):1216–1221
- Wang Z, Jiang H, Chen S, Du F, Wang X (2012) The mitochondrial phosphatase PGAM5 functions at the convergence point of multiple necrotic death pathways. *Cell* 148(1–2):228–243
- Wang H, Sun L, Su L, Rizo J, Liu L, Wang LF et al (2014) Mixed lineage kinase domain-like protein MLKL causes necrotic membrane disruption upon phosphorylation by RIP3. *Mol Cell* 54(1):133–146
- Wu JH, Mulatibieke T, Ni JB, Han X, Li B, Zeng Y et al (2017) Dichotomy between receptor-interacting protein 1- and receptor-interacting protein 3-mediated necroptosis in experimental pancreatitis. *Am J Pathol* 187(5):1035–1048
- Xie T, Peng W, Yan C, Wu J, Gong X, Shi Y (2013) Structural insights into RIP3-mediated necroptotic signaling. *Cell Rep* 5(1):70–78

Authors and Affiliations

Can Yu¹ · Zhao Lei² · Xia Li³ · Li-Hua Huang⁴ · Zhi-Qiang Li² · Hong-Wei Zhu² · Duo Han² · Hui Huang² · Xiao Yu² 

¹ Departments of Intensive Care Unit, Third Xiangya Hospital, Central South University, Changsha 410013, Hunan Province, People's Republic of China

² Departments of Hepatopancreatobiliary Surgery, Third Xiangya Hospital, Central South University, No. 138 Tongzipo Road, Yuelu District, Changsha 410013, Hunan Province, People's Republic of China

³ Departments of Endocrinology, Third Xiangya Hospital, Central South University, Changsha 410013, Hunan Province, People's Republic of China

⁴ Center for Medical Experiments, Third Xiangya Hospital, Central South University, Changsha 410013, Hunan Province, People's Republic of China